

# The Mu2e experiment at Fermilab: a search for lepton flavor violation

G. Pezzullo<sup>‡</sup>

INFN sezione di Pisa, Pisa, Italy

E-mail: pezzullo@pi.infn.it

**Abstract.** The Mu2e experiment at Fermilab will search for the charged lepton flavor violating process of neutrino-less  $\mu \rightarrow e$  coherent conversion in the field of an aluminum nucleus. About  $7 \cdot 10^{17}$  muons, provided by a dedicated muon beam line in construction at Fermilab, will be stopped in 3 years in the aluminum target. The corresponding single event sensitivity will be  $2.5 \cdot 10^{-17}$ . In this paper a brief overview of the physics explored by the  $\mu \rightarrow e$  conversion is given, followed by a description of the Mu2e experimental apparatus and the expected detector performance.

*Keywords:* Charged Lepton Flavor Violation Mu2e

<sup>‡</sup> on behalf of the Mu2e Collaboration [1]

## 1. Introduction

In the Standard Model (SM) version where only one Higgs doublet is included and massless neutrinos are assumed, lepton flavor conservation is an automatic consequence of gauge invariance and the renormalizability of the SM Lagrangian. However measurements of the neutrino mixing parameters during the last decades [2] showed that lepton flavor is not conserved. Including finite neutrino mass terms in the SM Lagrangian charged lepton flavor violation (CLFV) is also predicted. CLFV transitions are suppressed by sums over  $(\Delta m_{ij}^2/M_W^2)^2$ , where  $\Delta m_{ij}^2$  is mass-squared difference between the neutrino mass eigenstates  $i$ ,  $j$  and  $M_W$  is the  $W$  boson mass [3]. Because the neutrino mass difference is very small ( $\Delta m_{ij}^2 \leq 10^{-3} \text{eV}^2$  [2]) with respect to the  $W$  boson mass, the expected branching ratios reach values below  $10^{-50}$  [3, 4], which are unmeasurable by the present facilities. As a consequence, an observation of CLFV process would represent a clear evidence of new physics beyond the SM. In the last decades LFV processes were studied within the supersymmetric extensions of the SM (SUSY) [5, 3] and in particular within the supersymmetric grand unified theories (SUSY GUT) [6, 7]. In SUSY models there is a new source of flavor mixing in the mass matrices of SUSY partners for leptons and quarks, called sleptons and squarks respectively. Flavor mixing in the slepton mass matrix would induce LFV processes for charged leptons. In the SUSY GUT scenario, the flavor mixing in the slepton sector is naturally induced at the GUT scale because leptons and quarks belong to the same GUT multiplet [5]. In general, CLFV can be studied via a large variety of processes: muon decays, such as  $\mu^+ \rightarrow e^+\gamma$ ,  $\mu^\pm \rightarrow e^\pm e^- e^+$ , and muon conversion; tau decays:  $\tau^\pm \rightarrow \mu^\pm \gamma$ ,  $\tau^\pm \rightarrow \mu^\pm \mu^+ \mu^-$ , etc; meson decays:  $\pi^0 \rightarrow \mu e$ ,  $K_L^0 \rightarrow \mu e$ ,  $K^+ \rightarrow \pi^+ \mu^+ e^-$ , etc;  $Z^0$  decays, such as  $Z^0 \rightarrow \mu e$ , etc. The muon processes have been intensely studied in the CLFV for several reasons: low energy muon beams can be produced at high-intensity proton accelerator facilities; Final state of processes in the muon sector can be precisely measured. Search for CLFV with muons has been pursued looking for muon decays ( $\mu^+ \rightarrow e^+\gamma$  and  $\mu^\pm \rightarrow e^\pm e^- e^+$ ), and muon coherent conversion ( $\mu^- N \rightarrow e^- N$ ). A model-independent approach represents a convenient way to illustrate differences among these channels. CLFV can be introduced in the SM by adding CLF-violating terms to the SM Lagrangian [8]:

$$L_{CLFV} = \frac{m_\mu}{(\kappa + 1)\Lambda^2} \bar{\mu}_R \sigma_{\mu\nu} e_L F^{\mu\nu} + \text{h.c.} \\ + \frac{\kappa}{(\kappa + 1)\Lambda^2} \bar{\mu}_L \gamma_\mu e_L (\bar{e} \gamma^\mu e) + \text{h.c.},$$

where  $\Lambda$  is the mass scale of the new physics and  $\kappa$  is a dimensionless parameter. These two terms in the

equation above correspond to ‘‘dipole’’ and ‘‘contact’’ interactions terms, respectively, where  $m_\mu$  is the muon mass,  $F^{\mu\nu}$  is the electromagnetic field tensor, and  $R$  and  $L$  represent the chirality of the fermion fields. Figure 1 shows the  $\Lambda$  versus  $\kappa$  sensitivity plots for the

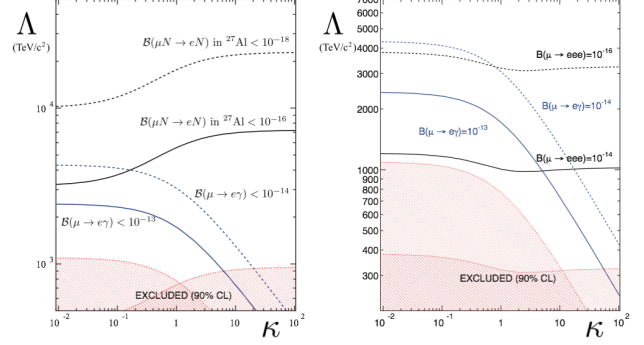


**Figure 1.**  $\Lambda$  versus  $\kappa$  sensitivity plots using:  $\mu^- N \rightarrow e^- N$  and  $\mu^+ \rightarrow e^+\gamma$  (left) and  $\mu^\pm \rightarrow e^\pm e^- e^+$  and  $\mu^+ \rightarrow e^+\gamma$  branching ratios. Red filled areas represent the region already excluded @ 90 CL.

CLFV muon channels. These plots also show that:

- $\mu^- N \rightarrow e^- N$  search can explore the phase space region where the contact term is dominant and  $\mu^+ \rightarrow e^+\gamma$  decay is further suppressed;
- The CLFV searches shown here are able to explore new physics mass scales significantly beyond the direct reach at the LHC energies.

Even if LHC discovers new physics in the second run, precise measurements of CLFV processes can help discriminate among several theoretical models [4].

Experimentally, the search of CLFV using rare muon decays presents pros and cons. One advantage comes from the fact that these processes are charge symmetric, so using either  $\mu^+$  or  $\mu^-$  has no theoretical disadvantage. However the use of positive muons reduces significantly the background sources thanks to the absence of capture processes. Nuclear captures are usually noisy for the detectors because they produce charged and neutral secondaries:  $p$ ,  $n$  and  $\gamma$ . On the other hand, channels involving  $\mu^+$  decays ( $\mu^+ \rightarrow e^+\gamma$ ,  $\mu^\pm \rightarrow e^\pm e^- e^+$ ) suffer for accidental background caused by the coincidence of two separate processes that can mimic the signal. This kind of background limits the beam intensity of the experiment.

## 2. Experimental searches for $\mu^- N \rightarrow e^- N$

When negative muons are stopped in a target (‘‘stopping target’’) they are quickly captured by the atoms ( $\sim 10^{-10}$  s) and cascade down to 1S orbital. Then muons can undergo the following processes:

decay in orbit (DIO)  $\mu^- \rightarrow e^- \nu_\mu \bar{\nu}_e$ ; weak capture  $\mu^- p \rightarrow \nu_\mu n$ ; coherent flavor changing conversion  $\mu^- N \rightarrow e^- N$ . The muon conversion represents a powerful channel to search for CLFV, because it is characterized by a distinctive signal consisting in a mono-energetic electron with energy  $E_{ce}$ :

$$E_{ce} = m_\mu - E_b - \frac{E_\mu^2}{2m_N},$$

where  $m_\mu$  is the muon mass at rest,  $E_b \sim Z^2 \alpha^2 m_\mu / 2$  is the muonic atom binding energy for a nucleus with atomic number  $Z$ ,  $E_\mu$  is the nuclear recoil energy,  $E_\mu = m_\mu - E_b$ , and  $m_N$  is the atomic mass [3]. In case of aluminum, which is the major candidate for upcoming experiments,  $E_{ce} = 104.973$  MeV [9]. In muon conversion experiments the quantity:

$$R_{\mu e} = \frac{\Gamma(\mu^- + N \rightarrow e^- + N)}{\Gamma(\mu^- + N \rightarrow \text{all captures})}$$

is measured. The normalization to captures offers a calculation advantage since many details of the nuclear wavefunction cancel in the ratio [9].

The coherent conversion leaves the nucleus intact, and there is only one detectable particle in the final state. The resulting electron energy stands out from the background (this will be more clear in the next paragraph), hence muon-electron conversion does not suffer from accidental background, and extremely high rates can be used.

### 2.1. Background sources

$\mu^-$  stopped in the stopping target can undergo a nuclear capture [10]. Particles generated in the muon capture (n, p and  $\gamma$ ) may reach the detector system, and create extra activity that can either obscure a conversion electron (CE) track or create spurious hits. As a result, some specific shielding is required to reduce this background. Additional shielding is required against cosmic rays that can interact in the apparatus, producing electrons with an energy mimicking a CE.

Electrons from the high momentum tail of the muon DIO represent the largest background source for the  $\mu^- N \rightarrow e^- N$  search. Figure 2 shows the energy spectrum of DIO electrons [11]. The main features

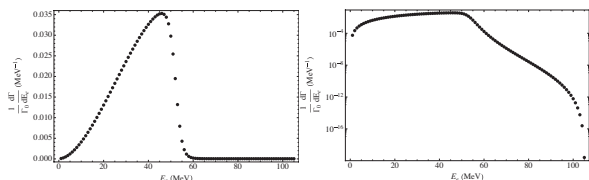


**Figure 2.** DIO electron energy spectrum on linear (left) and log (right) scale, for muons bounded in aluminum nuclei.

of the DIO energy spectrum can be summarized as follows:

- the endpoint of the spectrum corresponds to the energy of the electrons from  $\mu^- N \rightarrow e^- N$  conversion (CE);
- the overall spectrum is falling as  $(E_{ce} - E_e)^5$ , where  $E_{ce}$  is the CE energy, and  $E_e$  is the DIO energy;
- about  $10^{-17}$  of the spectrum is within the last MeV from the endpoint.

Therefore, to reach a sensitivity at the level  $O(10^{-17})$  the detector resolution is crucial.

Another relevant background comes from the radiative pion capture (RPC) process  $\pi^- N \rightarrow \gamma N^*$ , followed by the electron-positron pair conversion of the  $\gamma$ . Another source of background are pions; muon beam is generated from low energy protons (below 10 GeV of energy) interacting with a (production) target, so producing charged pions that then decay in a transport line. Unfortunately not all pions decay in the transport line, and, consequently, the muon beam is contaminated by pion. This source of background is reduced thanks to the difference between the pion and the bound muon life times. The pion has a  $\tau < \text{few tens of ns}$ , while the bound muon has a mean lifetime of the order of several hundreds of ns (depending on the  $Z$  of the material [10]). Therefore using a pulsed beam structure, it is possible to define a live-gate delayed with respect to the beam arrival, and to reduce the  $\pi^- N \rightarrow \gamma N^*$  contribution to the desired level. Other beam-related sources of background are: remnant electrons in the beam that scatter in the stopping target, muon decays in flight, and antiprotons annihilating in or near the stopping target.

## 3. Experimental technique

The Mu2e experiment had its genesis back in the 80s, behind the Iron Curtain. In a way, Mu2e was born in the Soviet Union. In 1989, the Soviet Journal of Nuclear Physics published a letter to the editor from physicists Vladimir Lobashev and Rashid Djilkibaev, where they proposed an experiment that would perform the most thorough search yet for muon-to-electron flavor violation. In 1992, they proposed the MELC experiment at the Moscow Meson Factory [12], but then, due to the political and economic crisis, in 1995 the experiment shut down. The same overall scheme was subsequently adopted in the Brookhaven National Laboratory MECO proposal in 1997 [13]. The Mu2e experimental apparatus includes three main superconducting solenoid systems:

- **Production solenoid (PS)**, where an 8 GeV pulsed proton beam strikes a tungsten target,

producing mostly pions;

- **Transport solenoid (TS)**, allowing to select low momenta negative pions coming from the production solenoid and letting them to decay into muons before they reach the detector region;
- **Detector solenoid (DS)**, housing the aluminum muon stopping target and the detector system.

Downstream to the proton beam pipe, outside the PS, an extinction monitor is used to measure the number of protons in between two subsequent proton pulses. The DS is surrounded by a cosmic ray veto system, which covers the DS from three sides (the ground is not covered) and extends up to the midpoint of the TS. Outside the DS, a stopping target monitor is used to measure the total number of muon captures. Figure 3 shows the Mu2e experimental apparatus.

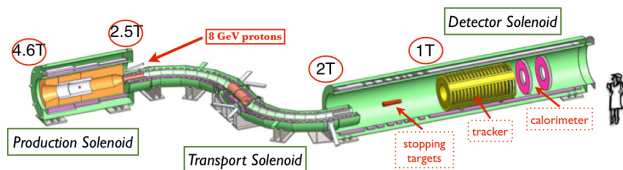


**Figure 3.** Mu2e apparatus.

The Mu2e detector consists of a low-mass straw tube tracker and a crystal electromagnetic calorimeter. The tracker is assembled of 5 mm diameter straw tubes. The straws are made of 15  $\mu\text{m}$  thick metalized Mylar and have 25  $\mu\text{m}$  sense wires. The tracker has about 20k straws combined in 18 tracking stations over a total length of about 3 m [14]. The straw tubes are orthogonal to the DS axis, and occupy an annulus with radii from 36 to 70 cm. Two layers of straws form a panel, 6 panels rotated with respect to each other form a plane, and a tracking station is made of two rotated planes. Only a small fraction of the DIO electrons fall into the tracker acceptance. The inner radius of the tracker planes is such that only electrons with energies greater than about 53 MeV fall into the tracker volume: lower energy electrons curl in the solenoidal field and pass unobstructed through the hole in the center of the tracker. Because most of the electrons have energy smaller than 60 MeV, a large fraction of them (97%) do not reach the tracker. The momentum resolution is pivotal for eliminating the background, and it is required to be better than few hundreds of keV/c [14]. The calorimeter consists of two disks with an inner (outer) radius of 37.4 (66) cm, and a relative distance of 75 cm. Each disk is composed of about 600 pure CsI crystals read out by Silicon Photomultipliers. The crystal size is  $3.4 \times 3.4 \times 20 \text{ cm}^3$ . Simulation studies and beam tests with a reduced scale prototype [15] showed that the calorimeter performance for 100 MeV

electrons are: a timing resolution of about 100 ps, and an energy resolution of about 5%. Calorimeter information allows to improve track reconstruction, and to provide a particle identification tool. The calorimeter may also be used to trigger high energy electron candidates, reducing the throughput of the data acquisition system. A cosmic ray veto system is also present to veto atmospheric muons that can interact in the DS, generating fake CE candidates. Figure 4 shows the signal and the DIO background

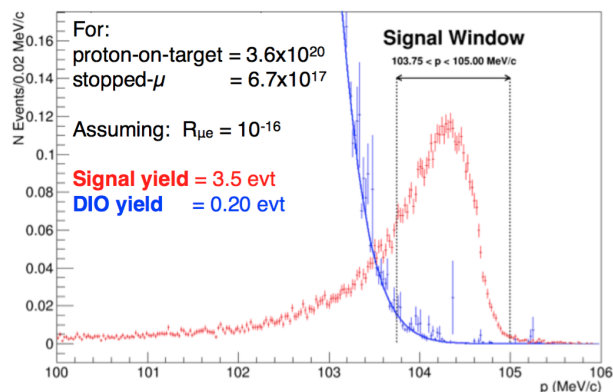


**Figure 4.** Signal and DIO background yield normalized to 3 years of Mu2e data taking.

yield, normalized to 3 years of data taking. Same Figure shows that if we define a narrow momentum window (signal window) around the signal peak, the mean expected background from the DIO electrons is about 0.2 events, while assuming  $R_{\mu e} = 10^{-16}$  the signal yield is expected to be about 3.5 events. It has also been shown in reference [14] that the contribution from the other background sources adds 0.3 events in the signal window.

#### 4. Summary

The Mu2e experiment will search for the  $\mu \rightarrow e$  conversion in the field of an aluminum nucleus with a single event sensitivity of  $2.9 \cdot 10^{-17}$ . This will improve the current best limit by 4 orders of magnitude, probing new physics at scales up to 10,000 TeV. The detector system consists of a low-mass straw tube tracker that will measure the signal momentum with an expected resolution better than 200 keV/c, and a crystal calorimeter made of pure CsI that will measure the energy (time) of the signal particle with a resolution of about 5% (100 ps). The design of the apparatus is mature and the construction of several components is underway to start data taking in the end of 2020.

## Acknowledgments

We are grateful for the vital contributions of the Fermilab staff and the technical staff of the participating institutions. This work was supported by the US Department of Energy; the Italian Istituto Nazionale di Fisica Nucleare; the US National Science Foundation; the Ministry of Education and Science of the Russian Federation; the Thousand Talents Plan of China; the Helmholtz Association of Germany; and the EU Horizon 2020 Research and Innovation Program under the Marie Skłodowska-Curie Grant Agreement No.690385. Fermilab is operated by Fermi Research Alliance, LLC under Contract No. De-AC02-07CH11359 with the US Department of Energy.

## References

- [1] Mu2e Collaboration, <http://mu2e.fnal.gov/collaboration.shtml>
- [2] Olive, K. and others, *Review of Particle Physics*, Chin. Phys., C38, 2014
- [3] Marciano, W. J. and others, *Charged Lepton Flavor Violation Experiments*, Annual Review of Nuclear and Particle Science, 58, 1, 315-341, 2008
- [4] Cei, F. and Nicolo, D., *Lepton Flavour Violation Experiments*, Adv. High Energy Phys., 2014, 2014
- [5] Kuno, Y. and Okada, Y., *Muon decay and physics beyond the standard model*, Rev. Mod. Phys., 73, 1, 151-202, 2001
- [6] Barbieri, R. and Hall, L. J., *Signals for supersymmetric unification*, Phys. Lett., B338, 1994
- [7] Barbieri, R. and Hall, L. J. and Strumia, A., *Violations of lepton flavor and CP in supersymmetric unified theories*, Nucl. Phys., B445, 1995
- [8] de Gouvea, A. and Vogel, P., *Lepton Flavor and Number Conservation, and Physics Beyond the Standard Model*, Prog. Part. Nucl. Phys., 71, 2013
- [9] Kitano, R. and Koike, M. and Okada, Y., *Detailed calculation of lepton flavor violating muon electron conversion rate for various nuclei*, Phys. Rev., D66, 2002
- [10] Measday, D. F., *The nuclear physics of muon capture*, Phys. Rept., 354, 2001
- [11] Czarnecki, A. and Garcia i Tormo, X. and Marciano, W.J., *Muon decay in orbit: Spectrum of high-energy electrons*, Phys. Rev., D84, 1, 8, 2011
- [12] Dzhilkibaev, R. M. and Lobashev, V. M., *The solenoid muon capture system for the MELC experiment*, Beam Dynamics and Technology Issues for mu+ mu- Colliders: Proceedings of the 9th ICFA Advanced Beam Dynamics Workshop, Oct. 15-20 1995, Montauk, New York, 1995
- [13] Popp, James L., *The MECO experiment: A Search for lepton flavor violation in muonic atoms*, Nucl. Instrum. Meth., A472, 354-358, 2000
- [14] Bartoszek, L. and others, *Mu2e Technical Design Report*, arXiv:1501.05241, [physics.ins-det], 2014
- [15] Pezzullo, G., *The Mu2e crystal calorimeter and improvements in the  $\mu^- N \rightarrow e^- N$  search sensitivity*, FERMILAB-THESIS-2016-02, 2016